Synthesis and Potent Antifolate Activity and Cytotoxicity of B-Ring Deaza Analogues of the Nonpolyglutamatable Dihydrofolate Reductase Inhibitor N α -(4-Amino-4-deoxypteroyl)- N δ...

ARTICLE *in* JOURNAL OF MEDICINAL CHEMISTRY · JANUARY 1999

Impact Factor: 5.45 · DOI: 10.1021/jm980477+ · Source: PubMed

9 AUTHORS, INCLUDING:

Andre Rosowsky
Dana-Farber Cancer Institute
292 PUBLICATIONS **5,469** CITATIONS
SEE PROFILE

Jorge Pardo
The Immune Tolerance Network
9 PUBLICATIONS **251** CITATIONS
SEE PROFILE

Synthesis and Potent Antifolate Activity and Cytotoxicity of B-Ring Deaza Analogues of the Nonpolyglutamatable Dihydrofolate Reductase Inhibitor N^{α}-(4-Amino-4-deoxypteroyl)-N^{δ}-hemiphthaloyl-L-ornithine (PT523)

Andre Rosowsky,* Joel E. Wright, Chitra M. Vaidya, Henry Bader, Ronald A. Forsch, Clara E. Mota, Jorge Pardo, Cindy S. Chen, and Ying-Nan Chen

Dana-Farber Cancer Institute and Department of Biological Chemistry and Molecular Pharmacology, Harvard Medical School, Boston, Massachusetts 02115

Received August 17, 1998

Six new B-ring analogues of the nonpolyglutamatable antifolate N^{α}-(4-amino-4-deoxypteroyl)-N^{δ}-hemiphthaloyl-L-ornithine (PT523, **3**) were synthesized with a view to determining the effect of modifications at the 5- and/or 8-position on dihydrofolate reductase (DHFR) binding and tumor cell growth inhibition. The 5- and 8-deaza analogues were prepared from methyl 2-L-amino-5-phthalimidopentanoate and 4-amino-4-deoxy-N^{10}-formyl-5-deaza- and -8-deazapteroic acid, respectively. The 5,8-dideaza analogues were prepared from methyl 2-L-[(4-aminobenzoyl)-amino]-5-phthalimidopentanoate and 2,4-diaminoquinazoline-6-carbonitriles. The K_i for inhibition of human DHFR by the 5-deaza and 5-methyl-5-deaza analogues was about the same as that of **3** (0.35 pM), 11-fold lower than that of aminopterin (AMT, **1**), and 15-fold lower than that of methotrexate (MTX, **2**). However the K_i of the 8-deaza analogue was 27-fold lower than that of **1**, and that of the 5,8-dideaza, 5-methyl-5,8-dideaza, and 5-chloro-5,8-dideaza analogues was approximately 50-fold lower. This trend was consistent with the published literature on the corresponding DHFR inhibitors with a glutamate side chain. In colony formation assays against the human head and neck squamous carcinoma cell line SCC25 after 72 h of treatment, the 5- and 8-deaza analogues were approximately as potent as **3**, whereas the 5,8-dideaza analogue was 3 times more potent. 5-Methyl and 5-chloro substitution was also favorable, with the 5-methyl-5-deaza analogue being 2.5-fold more potent than the 5-deaza analogue. However the effect of 5-methyl substitution was less pronounced in the 5,8-dideaza analogues than in the 5-deaza analogues. The 5-chloro-5,8-dideaza analogue of **3** was the most active member of the series, with an $IC_{50} = 0.33$ nM versus 1.8 nM for **3** and 15 nM for MTX. The 5-methyl-5-deaza analogue of **3** was also tested at the National Cancer Institute against a panel of 50 human tumor cell lines in culture and was consistently more potent than **3**, with IC_{50} values in the low-nanomolar to subnanomolar range against most of the tumors. Leukemia and colorectal carcinoma cell lines were generally most sensitive, though good activity was also observed against CNS tumors and carcinomas of the breast and prostate. The results of this study demonstrate that B-ring analogues of **3** inhibit DHFR activity and tumor cell colony formation as well as, or better than, the parent compound. In view of the fact that **3** and its B-ring analogues cannot form polyglutamates, their high cytotoxicity relative to the corresponding B-ring analogues of AMT is noteworthy.

Side-chain analogues of aminopterin (AMT, **1**), methotrexate (MTX, **2**), and other classical inhibitors of dihydrofolate reductase (DHFR) in which the L-glutamate moiety is replaced by a different, nonpolyglutamatable amino acid have been known for many years, but their clinical potential has thus far been largely unexplored (reviewed in ref 1). There has been a renewal of interest in such compounds recently because of the possibility that their lack of ability to form γ-polyglutamyl conjugates may reduce systemic toxicity. For example, it has been suggested that nonpolyglutamated analogues of MTX might be therapeutically useful for long-term, low-dose treatment of severe rheumatoid arthritis and other autoimmune disorders such as lupus erythematosus.[2,3] It had already been proposed earlier that compounds of this type might find a role in the treatment of tumors with low folylpolyglutamate synthetase activity.[4] Use of polyglutamatable antifolates against cells with this phenotype results in unfavorable selectivity. Examples of solid tumor cells with inefficient MTX polyglutamation include soft-tissue sarcomas,[5] head and neck squamous cell carcinomas,[6] and cervical squamous cell carcinomas.[7] Defective polyglutamation has likewise been correlated with poor response to MTX in certain forms of leukemia.[8]

An exceptionally potent nonpolyglutamatable analogue of AMT which has been investigated extensively by our group over the past several years is N^{δ}-(4-amino-4-deoxypteroyl)-N^{δ}-hemiphthaloyl-L-ornithine (PT523, **3**).[9] Because most of the structural features of the classical antifolates, including the α-carboxyl group, are retained, **3** is actively transported into cells via the reduced folate carrier (RFC).[10] It is also possible that some **3** may enter cells by routes other than the RFC.[11] The side chain in **3** is slightly longer than that of the classical antifolates, and recent high-field protein NMR[12]

10.1021/jm980477+ CCC: $15.00
Published on Web 11/25/1998

and crystallographic[13] studies of its ternary complex with NADPH and human DHFR indicate that the additional phenyl group at the end of the chain makes hydrophobic contacts within the active site. The extra phenyl group may also contribute to the more efficient uptake of **3** by the RFC. It should be noted that, since it cannot form polyglutamates, **3** can be thought of as being mechanistically related to 'small-molecule' antifolates, which likewise cannot form polyglutamates. However, in contrast to lipophilic nonpolyglutamated antifolates, **3** is much more soluble in water and thus is easily administered parenterally. Moreover, because **3** contains two ionized carboxyl groups, its accumulation in tumor cells, unlike that of the lipophilic DHFR inhibitors trimetrexate or piritrexim,[14] is not likely to be affected by overexpression of multidrug resistance (MDR) genes. To underscore these distinctions we recently proposed that nonpolyglutamatable antifolates should be divided into two categories, with type A consisting of the compounds traditionally designated as 'small-molecule antifols' and type B consisting of molecules with the overall appearance of classical antifolates but a nonpolyglutamatable side chain in place of L-glutamate.[1] According to this definition, small-molecule antifols would belong to type A, whereas PT523 would belong to type B.

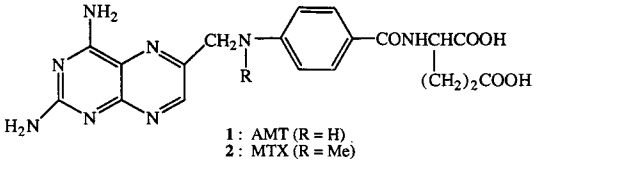

1: AMT (R = H)
2: MTX (R = Me)

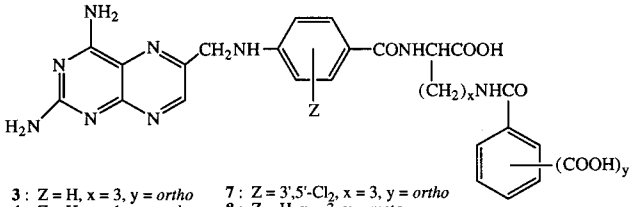

3: Z = H, x = 3, y = *ortho*
4: Z = H, x = 1, y = *ortho*
5: Z = H, x = 2, y = *ortho*
6: Z = H, x = 4, y = *ortho*
7: Z = 3',5'-Cl_2, x = 3, y = *ortho*
8: Z = H, x = 3, y = *meta*
9: Z = H, x = 3, y = *para*

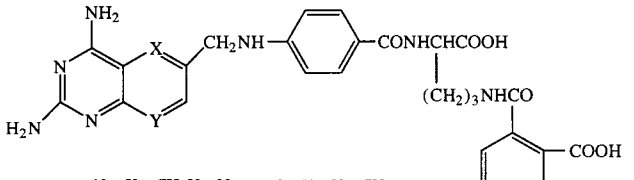

10: X = CH, Y = N
11: X = CMe, Y = N
12: X = N, Y = CH
13: X = Y = CH
14: X = CMe, Y = CH
15: X = CCl, Y = CH

As part of a broader effort to identify the structural features responsible for the unusually potent in vitro antitumor activity of PT523, we recently synthesized analogues of PT523 in which the number of CH_2 groups in the side chain was either shortened (**4**, **5**) or lengthened (**6**).[15] Also synthesized were the 3′,5′-dichloro analogue **7** and the isophthaloyl and terephthaloyl analogues **8** and **9**.[15] While substitution on the *p*-aminobenzoyl moiety and addition of an extra CH_2 group in the side chain were well-tolerated, shortening of the side chain and also moving the aromatic carboxyl group away from the ortho position of the phthaloyl moiety were markedly unfavorable. The finding that **3** was better than its isophthaloyl and terephthaloyl analogues suggested that restricted rotation of the phenyl ring via hydrogen bonding between the *o*-carboxyl group and the neighboring phthaloyl CONH group might be an important feature for uptake and/or DHFR binding. In the present paper we report the synthesis of six new analogues (**10**−**15**) in which we modified the B-ring with a view to determining how this structural change affects DHFR binding and tumor cell growth and how these type B nonpolyglutamatable analogues compare in potency with the corresponding glutamate analogues. A novel aspect of our series of hemiphthaloyl analogues is that it allows the effect of DHFR inhibition on cell growth to be viewed independently of a cell's ability to form polyglutamates that can inhibit enzymes other than DFHR, such as thymidylate synthase and/or aminoimidazolecarboxamide ribonucleotide formyltransferase.[16] As discussed below, all the hemiphthaloylornithine analogues proved to be exceptionally potent DHFR inhibitors, with the best of them giving K_i values in the 0.1 pM range. Moreover, all of the analogues were more active than **3** against human tumor cells in culture. Thus, in contrast to changes in the side chain, changes in the B-ring in **3** are well-tolerated and result in increased potency.

Scheme 1[a]

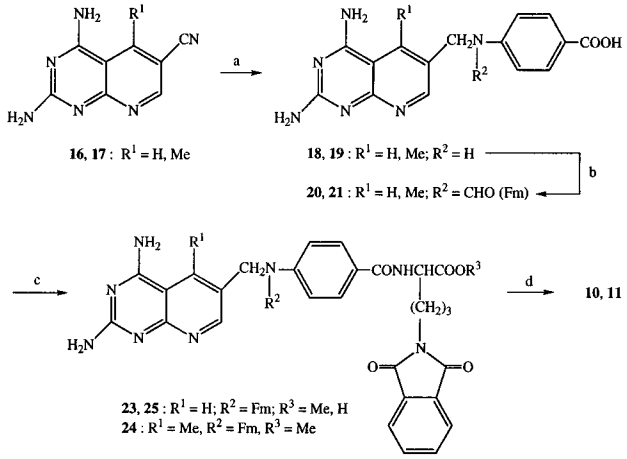

16, **17**: R^1 = H, Me
18, **19**: R^1 = H, Me; R^2 = H
20, **21**: R^1 = H, Me; R^2 = CHO (Fm)
23, **25**: R^1 = H; R^2 = Fm; R^3 = Me, H
24: R^1 = Me, R^2 = Fm, R^3 = Me

[a] Reagents: (a) 4-$H_2NC_6H_4COOH/H_2$-RaNi/AcOH; (b) HCOOH; (c) (i) *i*-BuOCOCl/Et_3N/DMF, (ii) methyl 2-L-amino-5-phthalimidopentanoate (**22**); (d) NaOH/DMSO.

Chemistry

The synthesis of the 5-deaza and 5-methyl-5-deaza analogues **10** and **11** (Scheme 1) is patterned after the one we had already used to prepare the corresponding 5-unsubstituted N^{δ}-Cbz analogue.[17] The 2,4-diaminopyrido[2,3-*d*]pyrimidine-6-carbonitriles **16** and **17**[18] were subjected to a reductive amination reaction with 4-aminobenzoic acid in the presence of Raney nickel, and the coupling products **18** and **19**[19] were converted directly to the N^{10}-formyl derivatives **20** and **21** by heating with 95−97% formic acid. Condensation of the N^{10}-protected intermediates with methyl L-2-amino-5-phthalimidopentanoate (**22**) by the mixed anhydride method (*i*-BuOCOCl/Et_3N), using either three cycles of addition of the reactants in the case of **20** or a single addition in the case of **21**, yielded the phthalimido esters **23** and **24**. In the final step, brief warming for 5 min with NaOH in DMSO at room temperature resulted in

Scheme 2[a]

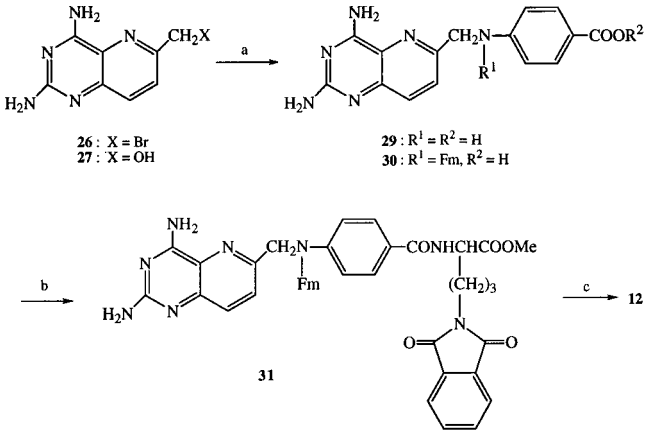

[a] Reagents: (a) (i) 4-$H_2NC_6H_4COOH$ (**28**), (ii) HCOOH; (b) (i) *i*-BuOCOCl/Et_3N/DMF, (ii) methyl 2-L-amino-5-phthalimidopentanoate (**22**); (c) NaOH/DMSO.

Scheme 3[a]

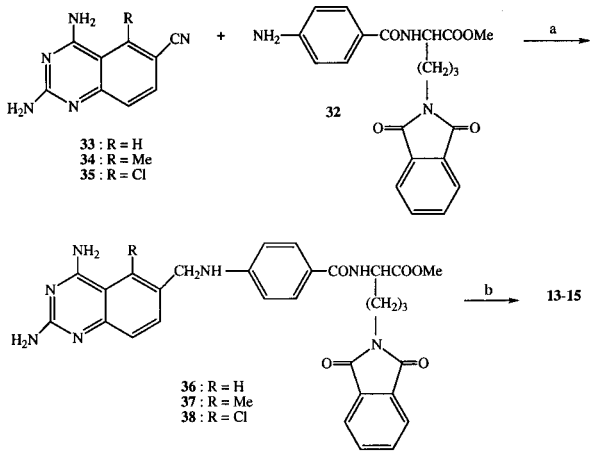

[a] Reagents: (a) H_2/RaNi/AcOH; (b) NaOH/DMSO.

simultaneous opening of the phthalimide ring and removal of the N^{10}-formyl and methyl ester protecting groups. The various blocked intermediates had the expected IR and NMR spectral properties but, because of their sparing solubility, had to be used with minimum purification. In the case of **23**, some formation of acid **25** was found to occur during column chromatography on silica gel when 85:15:1 $CHCl_3$−MeCN−28% NH_4OH was used as the eluent. Since the ester group would eventually have to be removed anyway, this did not pose a problem; however, to avoid premature loss of the methyl ester at this stage, column chromatography of **24** was performed with 5:5:2 $CHCl_3$−MeCN−MeOH as the eluent.

For the synthesis of the 8-deaza analogue **12** (Scheme 2), 2,4-diaminopyrido[3,2-*d*]pyrimidine hydrobromide (**26**·HBr) was freshly prepared from alcohol **27** and PBr_3 as described earlier[20,21] and allowed to react with 4-aminobenzoic acid (**28**) in DMF at room temperature for 5 days. The resultant product (**29**) was converted directly to the more soluble N^{10}-formyl derivative **30** by heating it with sodium formate in 98% formic acid. Further reaction of **30** with **22** (*i*-BuOCOCl/Et_3N/DMF), followed by alkaline hydrolysis (NaOH/DMSO), then gave the intermediate phthalimide ester **31** and the final product **12**. As in the synthesis of **10** and **11**, compounds **29**−**31** had the expected IR and NMR spectral features and were therefore used after only partial purification, consisting of DEAE-cellulose ion-exchange chromatography in the case of acid **30** and silica gel chromatography in the case of ester **31**. The final product **12** was purified to homogeneity by passing it twice through a DEAE-cellulose column.

For the synthesis of the 5,8-dideaza analogues **13**−**15** (Scheme 3), methyl 2-L-[(4-aminobenzoyl)amino]-5-phthalimidopentanoate (**32**)[15a] was reductively coupled to the known 2,4-diaminoquinazoline-6-carbonitriles **33**−**35**[22] in the presence of Raney nickel, and the resulting products (**36**−**38**) were treated with NaOH in DMSO under the usual conditions.

Enzyme Inhibition

The binding of B-ring-modified compounds **10**−**15** to human DHFR was evaluated by comparing their K_i values against human recombinant enzyme isolated from the high-expression *Escherichia coli* transfectant JM107 as described by Prendergast and co-workers.[23] The enzyme was electrophoretically pure, and its K_m with dihydrofolate as the substrate was confirmed to be 0.1 μM as reported earlier.[24] K_i values for the inhibitors, including the reference compounds AMT and MTX, were determined from Henderson-type plots[25] for tight-binding competitive inhibitors as described.[26] Examples of linearized plots obtained by this method are shown in Figure 1. As shown in Table 1, the average K_i of MTX from six independent experiments was found to be 5.19 ± 0.45 pM, a value consistent with that obtained earlier under the same assay conditions.[24] AMT, with a K_i of 3.70 ± 0.35 pM, was a somewhat better inhibitor than MTX, in agreement with the findings of Sirotnak and co-workers using mouse DHFR.[27]

All the B-ring analogues of **3** were potent inhibitors of human DHFR, with K_i values in the 0.1−0.4 pM range (Table 1). The K_i of **3** was roughly 10-fold lower than that of AMT and 15-fold lower than that of MTX. A statistically significant difference in K_i between **3**, the 5-deaza analogue **10**, and the 5-methyl-5-deaza analogue **11** was not observed. In constrast, the 8-deaza analogue **12** was a somewhat better inhibitor, with a K_i of 0.19 pM versus 0.35 pM for **3**.[12] Deletion of both B-ring nitrogens led to even tighter binding, with compounds **13**−**15** all giving K_i values in the 0.09−0.11 pM range, representing a roughly 50-fold difference relative to MTX and a 40-fold difference relative to AMT. As in the case of the 5-deaza compounds, the effect of substitution at the 5-position was negligible. Differences in basicity among the three diaminopyrimidine ring systems may partially explain the tighter binding of quinazolines **13**−**15** and the pyridopyrimidines **10**−**12** in comparison with **3**. However, as we have discussed elsewhere,[28] the pK_a differences among these compounds probably do not exceed 0.1−0.2 unit. Since such a small pK_a difference would probably not be enough by itself to account for the 4-fold difference in K_i between **3** and **13**, the improved binding of the quinazolines presumably reflects one or more physicochemical interactions that are not currently well-understood.

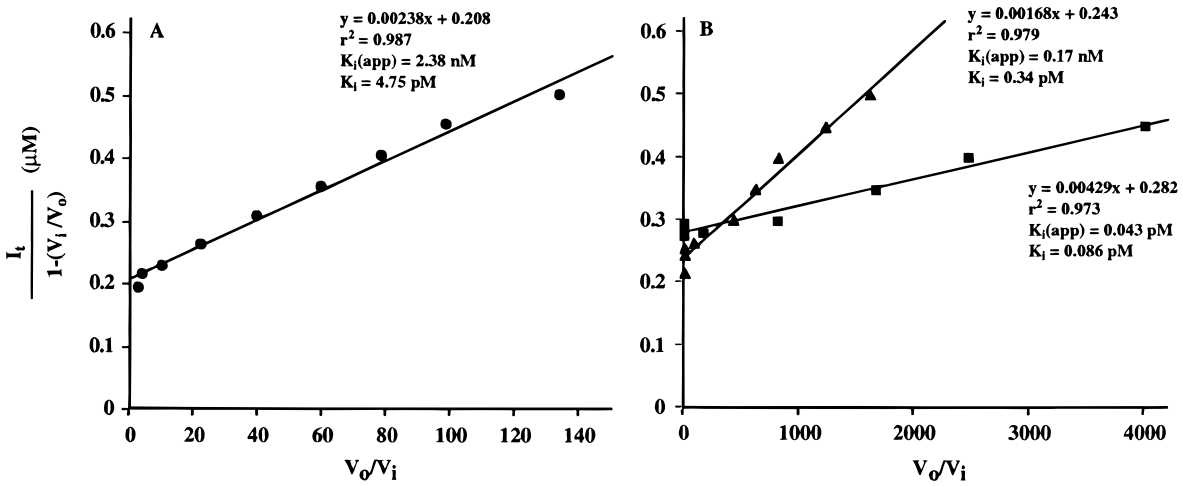

Figure 1. Representative examples of Henderson-type linearized plots of the kinetics of DHFR inhibition. According to this method of linearization, $I_t/1 - (V_i/V_o)$ is plotted against V_o/V_i, where I_t is the total concentration of inhibitor and V_i and V_o are the initial velocity in the presence and absence of inhibitor. The data were fitted to a straight line, and the slope and regression coefficient r^2 were determined with the aid of the software program Cricket III. The K_i was calculated from the equation $K_i = K_i(\text{app})/(1 + S/K_m)$, where K_i(app) is the slope, S is the dihydrofolate concentration, and K_m is the Michaelis−Menten constant for the reduction of dihydrofolate to tetrahydrofolate in the absence of inhibitor. Panel A: MTX (circles). Panel B: **3** (triangles) and **15** (squares). Note the different scales in the two panels. The K_i results given in Table 1 are averages of at least three replicate experiments performed on different days using the same batch of purified enzyme. Reactions were performed as described in Table 1, footnote a.

Table 1. Dihydrofolate Reductase Inhibition and in Vitro Antitumor Activity of B-Ring Analogues of **3**

compd	X	Y	DHFR (K_i, pM)[a]	cytotoxicity (IC_{50}, nM)[b]
MTX			5.19 ± 0.45 (1)	15 ± 2.2 (1)[c]
AMT			3.70 ± 0.35 (1.4)	*c*
3	N	N	0.35 ± 0.13 (15)	1.8 ± 0.51 (8)[c]
10	CH	N	0.41 ± 0.11 (13)	1.8 ± 0.19 (8)
11	CMe	N	0.40 ± 0.10 (13)	0.72 ± 0.21 (21)
12	N	CH	0.19 ± 0.006 (27)	1.2 ± 0.15 (13)
13	CH	CH	0.09 ± 0.03 (58)	0.61 ± 0.06 (25)
14	CMe	CH	0.10 ± 0.008 (52)	0.44 ± 0.16 (34)
15	CCl	CH	0.11 ± 0.05 (47)	0.33 ± 0.12 (45)

[a] K_i was determined from Henderson-type plots[25] for competitive inhibition as described earlier.[12] Titrations were performed at 22 °C in 0.05 M Tris HCl, pH 7.5, containing 0.15 M KCl, 65 μM NADPH, and 50 μM H_2PteGlu. Total inhibitor concentrations ranged from 0.15 to 0.50 μM. An experimentally determined value of 0.1 μM was used as the K_m of H_2PteGlu in the calculation of K_i.[12] Each K_i value listed is the mean ± SD from three or more assays performed on different days. Numbers in parentheses are normalized relative to MTX (1.0). [b] SCC25 human head and neck squamous carcinoma cells were exposed to different concentrations of drug for 72 h in 60-mm plates at 37 °C under a 5% CO_2 humidified atmosphere in Dulbecco's modified Eagle's medium supplemented with 10% fetal bovine serum and hydrocortisone (400 μg/mL). The cells were then replated at different densities depending on the drug concentration used, and after 10−14 days the colonies were stained with crystal violet and counted. Only colonies containing ≥50 cells were scored. Each IC_{50} value listed is the mean ± SD from three or more assays performed on different days. Numbers in parentheses are normalized relative to MTX (1.0). [c] IC_{50} values previously reported for MTX and AMT against SCC25 cells by this colony formation assay were 14 and 1.6 nM (single experiments).[35] When the growth of the cells was determined with sulforhodamine B after 72 h of drug exposure in 96-well plates,[30] the IC_{50} values (mean ± SD) obtained for MTX, AMT, and **3** were 22 ± 1.6, 7.7 ± 0.5, and 1.4 ± 0.15 nM.

Cell Growth Inhibition

A comparison of the ability of the various B-ring analogues of **3** to inhibit the growth of human SCC25 head and neck squamous carcinoma cells in culture is shown in Table 1 in addition to the DHFR data. The SCC25 cell line has been used previously in our laboratory to assess the growth inhibitory activity of other analogues of **3**.[9a,15,29] A colony formation assay was used, wherein the cells were exposed to drug for 72 h and, after being replated as single cells, were allowed to form colonies in drug-free medium over a period of 10−14 days. The IC_{50} values of the 5- and 8-deaza analogues **10** and **12** were in the 1−2 nM range, whereas the 5-methyl-5-deaza analogue **11** and the 5,8-dideaza analogues **13**−**15** were in the 0.3−0.6 nM range. Replacement of either N^5 or N^8 by carbon had little or no effect on cytotoxicity relative to **3**, whereas replacement of both ring nitrogens by carbon resulted in a roughly 3-fold increase in cytotoxicity. In addition, 5-methyl and 5-chloro substitution appeared to give a slight increase in cytotoxicity. The most cytotoxic member of the series was the 5-chloro analogue **15**, which was 5-fold more potent than **3** and 45-fold more potent than MTX. These results were generally consistent with the enzyme binding data and supported the conclusion that the major reason for the greater potency of B-ring analogues of **3** relative to the parent drug is an increased affinity for DHFR.

The 5-methyl-5-deaza analogue **11** was synthesized in sufficient amount to allow in vitro testing against the NCI panel of human tumor cell lines.[30] Assays were performed against a total of 50 cell lines including leukemias, CNS tumors, melanomas, and carcinomas of the lung, colon, kidney, ovary, breast, and prostate. These cell lines are very heterogeneous in their response to MTX, and the phenotypic basis for this variation in sensitivity has thus far been only partially characterized.[31] Results are summarized in Table 2, along with comparative data for **3** and MTX, some of which were presented earlier.[15b] IC_{50} values of 1 nM or less were obtained with **11** against all the leukemias and also against a majority of the solid tumor cell lines. The types of tumors exhibiting the best overall in vitro response to **11** were the leukemias and colon carcinomas, though several of the other carcinomas likewise gave IC_{50}

Table 2. In Vitro Activity of **11** versus **3** and MTX against Human Tumor Cells (NCI Panel)[a]

	IC_{50} (nM)		
cell lines	**11**	**3**	MTX
Leukemia			
CCRF-CEM	0.57	1.5	29
HL-60 (TB)	<1.0	0.41	39
K562	<0.1	0.30	26
MOLT-4	0.57	5.2	28
RPMI-8226	0.84	>100	33
SR	0.45	0.42	33
Lung			
A549/ATCC	0.42	0.57	33
EKVX	2.5	23	>1000
HOP-92	>1000	7.5	>1000
NCI-H226	0.62	>100	>1000
NCI-H23	1.5	2.6	43
NCI-H460	0.38	0.43	28
NCI-H522	1.5	6.5	450
Melanoma			
LOX IMV1	<0.1	0.23	26
MALME-3M	47	2.0	>1000
M14	0.66	>100	32
SK-MEL-2	>1000	>100	>1000
SK-MEL-28	190	4.6	>1000
SK-MEL-5	0.64	4.7	87
UACC-257	470	25	790
UACC-62	0.40	0.56	28
Ovary			
IGROV1	0.52	>100	65
OVCAR-3	17	46	400
OVCAR-4	>1000	>100	>1000
OVCAR-5	200	1.0	980
OVCAR-8	0.32	0.53	31
Colon			
COLO 205	6.7		870
HCC-2998	0.90	1.3	110
HCT-116	0.58	0.18	30
HCT-15	0.45	0.60	30
KM12	0.52	2.2	33
CNS			
SF-268	0.36	0.73	52
SF-295	0.59	0.51	36
SF-539	0.46	2.3	35
SNB-251	2.2	>100	>1000
U251	3.6	5.2	63
Prostate			
PC-3	<0.1	>100	27
DU-145	<1.0	9.5	45
Kidney			
786-0	<0.1	0.50	33
A498	>1000	>1000	>1000
ACHN	0.39	0.81	40
RXF-393	380	8.6	>1000
TK-10	>1000	9.6	>1000
Breast			
MCF7	0.70	3.6	36
NCI/ADR-RES	0.30	2.7	78
HS578T	100	>100	>1000
MDA-MB-435	0.60	3.1	>1000
BT-549	>1000	>100	>1000
T-47D	>1000	>100	>1000

[a] The cells were exposed to drug in 96-well plates for the last 48 h of a 72-h incubation and were then stained for total protein with sulforhodamine B according to the standard NCI protocol.[30] All the data were generously provided by the Developmental Therapeutics Program, National Cancer Institute. The data for **11** are from one experiment (ID #9707RC52-4), those for **3** against all the cell lines except the breast and prostate carcinomas are from another (ID #9009RC34), and those for **3** against the breast and prostate cell lines are from a third (ID #9510SR81). The data for MTX, kindly provided by Dr. Jeffrey Watthey (Starks C.P., Rockville, MD), are from the historical NCI data base and are the average values from at least 50 separate experiments per cell line.

values in the subnanomolar range. Three tumor lines had IC_{50} values in the 1−3 nM range even though they were highly resistant to MTX and/or **3**. Six tumors were less sensitive to **11** than to **3**, and five tumors were highly cross-resistant to both **11** and **3**, as well as to MTX. Overall, the results indicated that, while there was as much divergence in sensitivity to **11** as there was to **3** among the 50 cells in the NCI pannel, the IC_{50} of **11** was lower in almost every instance, sometimes by as much as 10-fold.

Discussion

The K_i values of the hemiphthaloylornithine analogues **10**−**15** as DHFR inhibitors are of interest to compare with those previously found with the corresponding glutamate analogues **39**−**44**. Thus, the K_i values of AMT, 5-deazaAMT (**39**), and 5-methyl-5-deazaAMT (**40**) are reported to be 3.55, 3.65, and 2.93 pM,[18] and in the 5,8-dideaza series the K_i values of 5,8-dideazaAMT (**42**), 5-methyl-5,8-dideazaAMT (**43**), and 5-chloro-5,8-dideazaAMT (**44**) are reported to be 0.6, 0.4, and 0.1 pM.[32] To our knowledge, a K_i for 8-deazaAMT (**41**)[33] has not been reported in the literature. From the available data on the 5-deaza and 5,8-dideaza compounds, there appear to be similarities between the various B-ring analogues of **3** and the corresponding glutamate derivatives. It is clear, for example, that 5,8-dideaza substitution has a favorable effect on binding and that this effect is more pronounced among the AMT analogues than among the analogues of **3**. However there is also a difference among the 5,8-dideaza compounds in the two series, in that the K_i values of the AMT analogues are more markedly influenced by the nature of the 5-substituent. Thus, while we were unable to demonstrate a statistically significant K_i difference between **13** and **15**, the reported difference between **42** and **44** is 6-fold, and a similar, though smaller, effect is observed among the 5-deaza analogues. Although it cannot be ruled out that these results reflect the fact that the B-ring analogues of **3** were assayed against human DHFR whereas those of AMT were assayed against the mouse enzyme, we believe that the lack of a K_i difference among the three 5,8-dideaza analogues of **3** indicates that, once the binding affinity becomes high enough through replacement of the glutamate moiety by hemiphthaloylornithine, other structural

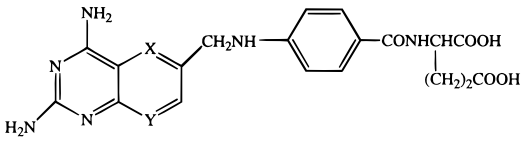

39: X = CH, Y = N
40: X = CMe, Y = H
41: X = N, Y = CH
42: X = Y = CH
43: X = CMe, Y = CH
44: X = CCl, Y = CH

factors (e.g., 5-substitution) become relatively less important.

Because the effect of different B-ring analogues of AMT on cell growth presumably reflects not only differences in transport and DHFR binding but also differences in polyglutamation, it was of interest to compare the IC_{50} values of the glutamate compounds

and the corresponding analogues of **3**. In one study using L1210 leukemia cells and a drug exposure time of 72 h, the IC_{50} values obtained for AMT, **39**, and **40** were 0.72, 0.63, and 0.13 nM, respectively.[18] Thus, as in the B-ring analogues of **3**, replacement of the nitrogen atom at the 5-position by carbon had very little effect on growth inhibitory potency. On the other hand, while 5-methylation of **3** had essentially no effect, there was a 5.5-fold increase in growth inhibitory potency in going from **39** to **40** which may reflect a difference in ability to undergo intracellular converson to long-chain polyglutamates (not a contributing factor in the case of the hemiphthaloylornithine analogues). That polyglutamation rather than transport is probably the major determinant of the differences in cell growth activity between AMT and its 5-deaza analogues is supported by the fact that the transport kinetics of these compounds are almost indistinguishable.[27]

In an independent study using L1210 cells but a 48-h treatment, the 5,8-dideazaAMT analogues **42**−**44** were found to have IC_{50} values of 21, 18, and 2.5 nM, respectively.[34] Thus, even after allowing for the fact that a shorter exposure time was used for the 5,8-dideaza analogues than for the 5-deaza analogues, the lower growth inhibitory potency of the 5,8-dideaza compounds is somewhat surprising since they are better DHFR inhibitors and are comparable to, if not better than, AMT itself in terms of polyglutamation.[35] On the other hand their transport kinetics are less favorable than those of AMT or the 5-deazaAMT analogues, suggesting that, where the 5,8-dideazaAMT analogues are concerned, differences in potency relative to AMT are more reflective of transport than of DHFR binding or polyglutamation. A notable feature of nonpolyglutamated analogues such as **3** is that growth inhibition can be assessed in terms of DHFR binding and transport alone, without the confounding effects that may be seen in antifolates as a result of polyglutamation.

In considering what the optimal binding characteristics for nonpolyglutamatable inhibitors should be, it may be noted that although the binding of AMT and MTX to DHFR is widely held to be nearly irreversible, there is in fact always some dissociation of the inhibitor from the active site at physiological pH. For this reason, a 15-fold increase in DHFR binding relative to MTX, such as we are seeing with **3**, may have a significant impact on cell growth. Kinetic analysis has shown, for example, that in cells where thymidylate synthesis is rate-limiting, DHFR activity has to be blocked by more than 98% in order to effectively shut down DNA synthesis.[26] Thus, in order for the DHFR to remain maximally inhibited in the face of an expanding pool of dihydrofolate, it is important to have some free, nonbound drug in the cell to minimize dissociation from the enzyme−inhibitor complex. The lower the K_i of the inhibitor, the smaller will be the amount of free drug needed to maintain >98% inhibition. In the case of classical antifolates such as MTX, this role is conveniently fulfilled by polyglutamation, since the polyglutamates have a negligible efflux rate while binding no less tightly to DHFR than the parent drug. In the case of a nonpolyglutamatable MTX analogue with a K_i similar to that of MTX, it would be possible to maintain the required amount of nonbound drug if transport is more efficient relative to MTX, i.e., when there is enough uptake to offset lack of MTX polyglutamation. On the other hand if the uptake of the nonpolyglutamated analogue is not substantially better than that of MTX, then the desired level of DHFR inhibition can be achieved only if there is less dissociation from the enzyme. In principle, the most favorable situation for a nonpolyglutamated analogue would be more efficient cellular uptake as well as better DHFR binding. As we recently demonstrated, **3** appears to combine both of these features.[10,12] Work is currently in progress to determine if B-ring analogues of **3** likewise display not only favorable DHFR binding characteristics but also efficient uptake kinetics relative to their glutamate counterparts.

Experimental Section

IR spectra were obtained on a Perkin-Elmer model 781 double-beam spectrophotometer and UV spectra on a Varian model 210 instrument. Kinetics of inhibition of human DHFR activity in the presence of the various inhibitors was performed on a Perkin-Elmer λ6 UV−visible spectrophotometer with a thermostatically controlled cell compartment as described in Table 1. ^{1}H NMR spectra were obtained at 60 MHz on a Varian EM360L spectrometer, with Me_4Si as the reference, or at 500 MHz on a Varian ML500 instrument. TLC analyses were performed on fluorescent Whatman MK6F silica gel coated microscope slides. Spots were visualized under 254-nm UV illumination, or with the aid of iodine or ninhydrin. Column chromatography was carried out on Baker silica gel (regular grade, 60−200 or 70−230 mesh; flash grade, 40-μm particle size) or on Whatman DE-52 preswollen DEAE-cellulose. Solvents for moisture-sensitive reactions were dried over Linde 4A molecular sieves. Analytical HPLC separations were on C_{18} silica gel radial compression cartridges (Waters, Milford, MA; analytical, 5-μm particle size, 5 × 100 mm; preparative, 15-μm particle size, 25 × 100 mm). Solid reaction products were generally dried in a vacuum oven or drying pistol under reduced pressure over P_2O_5 at 50−80 °C, in some instances after preliminary drying in a Labconco lyophilizer. Elemental analysis and ^{1}H NMR spectra showed that fractional molar amounts of organic solvents were tenaciously retained in some analytical samples even after prolonged drying under reduced pressure. Melting points (not corrected) were determined on a Fisher-Johns hot-stage microscope or in open Pyrex capillary tubes in a Mel-Temp apparatus (Cambridge Laboratory Devices, Cambridge, MA). Synthetic starting materials and other chemicals were purchased from Aldrich, Milwaukee, WI, or Fluka, Ronkonkoma, NY. Microanalyses were performed by Robertson Laboratory, Madison, NJ, and were within ±0.4% of theoretical values unless otherwise specified.

***N*$^{\alpha}$-[4-[*N*-[(2,4-Diaminopyrido[2,3-*d*]pyrimidin-6-yl)methyl]amino]benzoyl]-*N*$^{\delta}$-hemiphthaloyl-L-ornithine (10).** *i*-BuOCOCl (34 mg, 0.25 mmol) was added at room temperature to a stirred suspension of **20** (86 mg, 0.25 mmol)[18] in dry DMF (5 mL) containing Et_3N (202 mg, 2.0 mmol). After 20 min, methyl L-2-amino-5-phthalimidopentanoate hydrochloride (**22**·HCl)[15b] (78 mg, 0.25 mmol) was added. Stirring was continued for another 10 min, and a second portion of *i*-BuOCOCl (17 mg, 0.125 mmol) was added, followed 20 min later by a second portion of **22**·HCl (39 mg, 0.13 mmol). After 10 min, a third portion of *i*-BuOCOCl (9 mg, 0.062 mmol) was added, followed 20 min later by a third portion of **22**·HCl (20 mg, 0.062 mmol). After a final 15 min, the reaction was quenched with glacial AcOH (0.3 mL) and the solvents were removed under reduced pressure. The residue was dissolved in $CHCl_3$ (30 mL), and the solution was washed with H_2O, dried ($MgSO_4$), and evaporated to a solid, which was redissolved in $CHCl_3$ and chromatographed on a column of silica gel (flash grade, 10 g, 1 × 22.5 cm). The column was eluted with $CHCl_3$, then 5:5:2 $CHCl_3$−MeCN−MeOH, and finally 85:15:1 $CHCl_3$−MeOH−28% NH_4OH. Fractions recovered with

the last eluent showed a major TLC spot with R_f 0.28 (silica gel, 85:15:1 $CHCl_3$−MeOH−28% NH_4OH). Evaporation of these pooled fractions afforded a mixture of the ester **23** and acid **25** (80 mg): mp 153−156 °C.

A portion (49 mg) of the mixture of **23** and **25** was dissolved in DMSO (0.4 mL) and treated dropwise with 2.5 N NaOH (0.18 mL). After 5 min, the solution was diluted with H_2O (2 mL) and acidified to pH 4.3 with 1 N HCl (ca. 0.4 mL). The precipitate was filtered, washed with H_2O, dried on a lyophilizer, and finally kept under vacuum at 80 °C in the presence of P_2O_5 to obtain **10** as a pale-yellow solid (29 mg, 61%): mp 245−248 °C dec; IR (KBr) ν 3320, 3040, 2920, 1630, 1600, 1505, 1390, 1265, 1180, 830, 800, 760 cm^{-1}; UV (pH 7.4) λ_{max} 216 (ϵ 46 400), 246 (22 400), 279 (23 500), 294 infl (22 200) nm; ^1H NMR (DMSO-d_6) δ 1.60−1.88 (m, 4H, β- and γ-CH_2), 3.18 (m, 2H, δ-CH_2), 4.30 (m, 3H, 9-CH_2, α-CH), 6.62 (d, J = 8 Hz, 2H, 3′- and 5′-H), 6.65 (m, 1H, 10-H), 6.80 (m, 2H, NH_2), 7.37−7.80 (m, 6H, 2′-H, 6′-H, and phthaloyl), 7.92 (m, 2H, NH_2), 8.08 (m, 1H, phthaloyl CONH), 8.30 (m, 1H, benzoyl CONH), 8.44 (s, 1H, 5-H), 8.65 (s, 1H, 7-H). Anal. ($C_{28}H_{28}N_8O_6$·$2H_2O$) C, H, N.

Methyl 2-L-[[4-[*N*-[(2,4-Diamino-5-methylpyrido[2,3-*d*]pyrimidin-6-yl)methyl]-*N*-formylamino]benzoyl]amino]-5-phthalimidopentanoate (24). To a solution of nitrile **17** (1 g, 5 mmol)[18] in glacial AcOH (200 mL) were added H_2O (60 mL), 4-aminobenzoic acid (0.7 g, 5 mmol), and Raney Ni (1.5 g) which had been washed first with H_2O until the supernatant was neutral and then with 75% AcOH. The mixture was shaken under H_2 (40 psi initial pressure) in a Parr apparatus for 18 h and was then filtered through Celite. The filtrate was evaporated under reduced pressure, the residue was resuspended in H_2O (200 mL), the pH was adjusted to >12 by dropwise addition of 2 N NaOH, and a small amount of solid that remained undissolved was filtered off. The filtrate was adjusted to pH 4.5 with 10% AcOH, then concentrated to a small volume by rotary evaporation, and cooled on ice. The precipitate was collected, washed with H_2O, and dried to obtain acid **19** as a yellow-orange powder (0.46 g, 28%). Several batches of this product from different runs were pooled and used for the next step without purification.

A solution of crude **19** (2.8 g, 8.6 mmol) in 95−97% formic acid (90 mL) was kept in an oil bath at 75 °C for 2 h, then cooled to room temperature, and concentrated to dryness by rotary evaporation. The residue was treated with 10% NH_4OH (300 mL), the insoluble portion was filtered off, and the filtrate was acidified to pH 4.5 with 10% AcOH. The precipitated solid (**21**) was collected, washed with H_2O, dried, and used directly in the next reaction: yield 2.0 g (67%); mp 220 °C dec.

A suspension of **21** (500 mg, 1.42 mmol) in DMF (50 mL) containing Et_3N (287 mg, 2.84 mmol) was treated at room temperature with *i*-BuOCOCl (194 mg, 1.42 mmol) and 30 min later with **22** (440 mg, 1.42 mmol). After another hour of stirring, the solvent was removed by rotary evaporation and the residue was taken up in $CHCl_3$. The solution was washed with H_2O, the aqueous phase was back-extracted with $CHCl_3$, and the combined $CHCl_3$ layers were dried ($MgSO_4$) and evaporated. The residue was chromatographed in two batches on a silica gel column, using 5:5:2 $CHCl_3$−MeCN−MeOH to pack the column, apply the sample, and elute the product. Fractions with R_f 0.15 (silica gel, 100:10:1 $CHCl_3$−MeOH−28% NH_4OH) were pooled and evaporated. The residue was taken up in a minimum volume of 5:5:2 $CHCl_3$−MeCN−MeOH, and the solution was added dropwise to excess Et_2O. The precipitate was collected by centifugation, washed with H_2O, and dried, first by lyophilization and then in a vacuum oven at 60 °C in the presence of P_2O_5, to obtain the N^{10}-protected phthalimide ester **24** as a pale-yellow solid (170 mg, 20%): mp 215 °C, darkening at 180 °C. Anal. ($C_{31}H_{30}N_8O_6$·$0.4CHCl_3$) C, H, N.

N^{α}-[4-[*N*-[(2,4-Diamino-5-methylpyrido[2,3-*d*]pyrimidin-6-yl)methyl]amino]benzoyl]-N^{δ}-hemiphthaloyl-L-ornithine (11). A stirred solution of **24** (50 mg, 82 mmol) in DMSO (0.4 mL) was treated at room temperature with 2 N NaOH (0.26 mL), and the reaction mixture was stirred for 5 min, diluted with H_2O (6 mL), and adjusted to pH 4.3 with 10% AcOH. The precipitate was collected, washed with H_2O, and dried by lyophilization and then over P_2O_5 in a vacuum oven at 60 °C to obtain a pale-yellow powder (35 mg, 72%): mp >250 °C dec; TLC R_f 0.76 (5:4:1 $CHCl_3$−MeOH−28% NH_4OH); HPLC 8 min (C_{18} silica gel, 10% MeCN in 0.1 M NH_4OAc, pH 7.7, 1 mL/min); IR (KBr) ν 3350, 1630, 1600, 1500, 1370, 1270, 1190, 850, 800 cm^{-1}; UV (pH 7.4) λ_{max} 222 (ϵ 42 500), 282 (24 700) nm; ^1H NMR (DMSO-d_6) δ 1.51−1.89 (m, 4H, β- and γ-CH_2), 1.65 (s, 3H, 5-Me), 3.20 (m, 2H, δ-CH_2, mostly obscured by H_2O), 4.29 (m, 3H, α-CH and 9-CH_2), 6.52 (m, 1H, 10-NH), 6.62 (d, 2H, 3′- and 5′-H), 6.80 (broad s, 2H, NH_2), 7.35 (m, 1H, phthaloyl), 7.41−7.47 (m, 3H, phthaloyl), 7.67 (m, 2H, 2′- and 6′-H), 8.07 (m, 1H, benzoyl CONH), 8.30 (m, 1H, phthaloyl CONH), 8.48 (s, 1H, 7-H). A downfield signal corresponding to a second NH_2 group was not discernible in the δ 7.5−8.0 region for either **11** or its precursor **24** because of rapid exchange with H_2O. Anal. ($C_{28}H_{28}N_8O_6$·$2H_2O$) C, H, N.

Methyl 2-L-[*N*-[4-[*N*-[(2,4-Diaminopyrido[3,2-*d*]pyrimidin-6-yl)methyl]-*N*-formylamino]benzoyl]amino]-5-phthalimidopentanoate (31). 4-Aminobenzoic acid (685 mg, 5 mmol) was added to a solution of **26**·HBr (prepared by the PBr_3 method[20] from 191 mg, 1 mmol, of alcohol **27**) in dry DMF (5 mL). The mixture was stirred at room temperature for 5 days, the solvent was removed by rotary evaporation, and the residue was redissolved in a solution of sodium formate (340 mg, 5 mmol) in 98% formic acid (15 mL). The reaction mixture was refluxed for 30 min, and the solvent was removed under reduced pressure. The residue was taken up in 0.1 N NaOH; the solution was immediately adjusted to pH 7.8 with 0.1 N HCl and diluted with MeCN (ca. 10% v/v). Overnight refrigeration caused a solid to precipitate, which was collected and redissolved in 3% NH_4OH. Dilute HCl was added dropwise to pH 9, and the solution was applied onto a column of DEAE-cellulose (HCO_3^- form, 20 g, 1.5 × 28 cm). The column was eluted sequentially with H_2O to remove inorganic salts and with 0.1 M NH_4HCO_3 to remove an unknown impurity. Some product began to elute with 0.2 M NH_4HCO_3, but this was accompanied by substantial precipitation on the column. Thus, complete recovery required the use of a large volume (>300 mL) of 3% NH_4OH. Eluents containing mainly one TLC spot were pooled and lyophilized to obtain acid **30** as an off-white solid which was used directly for the next step: yield 155 mg (37%); mp >300 °C.

A stirred suspension of crude **30** (42 mg, 0.1 mmol) in dry DMF (3 mL) at room temperature was treated sequentially with Et_3N (12 mg, 0.12 mmol) and *i*-BuOCOCl (16 mg, 0.12 mmol). A clear solution formed in ca. 1 min. After another 15 min, **22** (38 mg, 0.12 mmol) was added, followed by another portion of Et_3N (12 mg, 0.12 mmol). Stirring was continued for 20 min, the solvent evaporated, and the residue chromatographed on silica gel (10 g, 1.5 × 15 cm). The column was eluted first with 20:1 $CHCl_3$−MeOH to remove a yellow impurity which did not absorb UV light and then with 10:1 $CHCl_3$−MeOH to remove a series of colorless fractions which were monitored by TLC and appropriately pooled. Evaporation of the pooled fractions to a small volume on the rotary evaporator, followed by cooling and dilution with Et_2O, yielded a precipitate. The solid was collected and dried in vacuo at 60 °C over P_2O_5 to obtain **31** as a white solid (37 mg, 54%): mp 151−157 °C, with prior softening. Anal. ($C_{30}H_{28}N_8O_6$·CH_3OH·$2.5H_2O$) C, H, N.

N^{α}-[4-[*N*-[(2,4-Diaminopyrido[3,2-*d*]pyrimidin-6-yl)methyl]amino]benzoyl]-N^{δ}-hemiphthaloyl-L-ornithine (12). A solution of **31** (81 mg, 0.136 mmol) in DMSO (3.5 mL) was treated with 2 N NaOH (0.255 mL, 0.510 mmol). Analytical HPLC (C_{18} silica gel, 10% MeCN in 0.05 M NH_4OAc, pH 6.9, 1.0 mL/min) showed the reaction to be almost complete after 5 min, as indicated by the emergence of a single new peak with an elution time of 9.5 min. The reaction mixture was diluted with H_2O (30 mL) and transferred to a DEAE-cellulose column (HCO_3^- form, 2.5 × 26 cm). Elution with H_2O,

0.2 M NH_4HCO_3, 0.4 M NH_4HCO_3, 0.4 M NH_4HCO_3 adjusted to pH 10 with 28% NH_4OH ("pH 10 buffer"), and finally 3% NH_4OH afforded several minor impurities which were discarded. Continued elution with 0.4 M NH_4HCO_3 (>1000 mL) followed by "pH 10 buffer" (500 mL) yielded a broad band containing the desired product. Lyophilization of this band, followed by drying in vacuo at 70 °C over P_2O_5, afforded a yellow solid (86 mg) whose elemental analysis indicated the presence of residual inorganic salt(s). Final purification was achieved by a second passage through DEAE-cellulose (HCO_3^- form, 1.5 × 13 cm) with 0.4 M NH_4HCO_3 as the eluent. Pooled TLC homogeneous fractions were freeze-dried to obtain a light-yellow solid whose analysis indicated it to be a partial ammonium salt (52 mg, 57%): mp 230 °C dec (softening at 190 °C); UV λ_{max} (pH 7.4) 218 (ϵ 49 700), 242 infl (24 800), 280 (23 500), 332 infl (8 000) nm; IR (KBr) ν 3350, 3220 sh, 2950 sh, 2860, 1640, 1610, 1575, 1510, 1450, 1390, 1310, 1280, 1190, 1135, 1095, 990, 840, 805, 770, 745, 695, 650 cm^{-1}; ^1H NMR (DMSO-d_6) δ 1.4−1.7 (m, 4H, β- and γ-CH_2), 3.1 (m, 2H, δ-CH_2 partly overlapped by DMSO-d_5 and H_2O), 4.35 (m, 1H, α-CH), 4.45 (s, 2H, 9-CH_2), 6.21 (m, 2H, NH_2), 6.7−7.8 (complex m, ca. 13H, 10-H, NH_2 and aromatic), 8.03 (broad s, 1H, phthaloyl CONH), 8.38 (broad s, 1H, benzoyl CONH). Anal. ($C_{28}H_{28}N_8O_6$·0.25NH_3·5H_2O) C, H, N.

Methyl 2-L-[*N*-[4-[*N*-[(2,4-Diaminoquinazolin-6-yl)methyl]amino]benzoyl]amino]-5-phthalimidopentanoate (36). A suspension of **32**[15a] (300 mg, 0.76 mmol), **33**[22] (420 mg, 2.27 mmol), and Raney Ni (0.4 g) in glacial AcOH (60 mL) was shaken under H_2 (1 atm) in a Parr apparatus for 18 h. The catalyst was removed by filtration through Celite, and the filter cake was washed with glacial AcOH. The combined filtrate and wash solution were concentrated to 15 mL under reduced pressure, then diluted with H_2O (50 mL), and adjusted to pH 9 with 28% NH_4OH. The brown precipitate was collected by centrifugation, washed with H_2O, dried in a lyophilizer, and chromatographed on silica gel (30 g, 2 × 28 cm) with 95:5 followed by 93:7 $CHCl_3$−MeOH as eluents. Fractions giving a single TLC spot with R_f 0.1 (silica gel, 100:10:1 $CHCl_3$−MeOH−28% NH_4OH) were pooled and evaporated. The residue was taken up in a small volume of 9:1 $CHCl_3$−MeOH, and the solution was added dropwise to a large volume of Et_2O. The precipitate was collected and dried in vacuo at 60 °C over P_2O_5 to obtain **36** as a pale-yellow powder (110 mg, 26%): mp 155 °C. Anal. ($C_{30}H_{29}N_7O_5$·0.9H_2O) C, H, N.

***N*$^{\alpha}$-[4-[*N*-[(2,4-Diaminoquinazolin-6-yl)methyl]amino]benzoyl]-*N*$^{\delta}$-hemiphthaloyl-L-ornithine (13).** To a solution of **36** (50 mg, 0.088 mmol) in DMSO (0.5 mL) was added 2 N NaOH (0.13 mL), and the mixture was stirred for 5 min, diluted with H_2O (7.5 mL), and adjusted to pH 4.2 with 10% AcOH. The precipitate was filtered, washed with H_2O (60 mL), and dried, first in a lyophilizer and then in vacuo at 60 °C over P_2O_5, to obtain a white powder (35 mg, 70%): mp 210 °C dec; HPLC 10 min (C_{18} silica gel, 10% MeCN in 0.1 M NH_4-OAc, pH 7.5, 1 mL/min); IR (KBr) ν 3340, 2950, 1650, 1610, 1530, 1450, 1400, 1310, 1220, 1190, 1130, 840, 770 cm^{-1}; UV λ_{max} (pH 7.4) 230 (ϵ 55 600), 296 (23 300) nm; ^1H NMR (DMSO-d_6) δ 1.51−1.91 (m, 5.8H, 0.6AcOH, β-CH_2, and γ-CH_2), 3.20−3.32 (m, 2H, δ-CH_2), 4.28 (m, 3H, α-CH and 9-CH_2), 6.57 (m, 2H, 3′- and 5′-H), 6.70 (m, 1H, 10-H), 7.27 (d, 1H, 7-H), 7.32 (d, 1H, 8-H), 7.40−7.42 (m, 3H, phthaloyl), 7.59 (m, 1H, phthaloyl), 7.60−7.65 (m, 2H, 2′- and 6′-H), 7.98 (m, 1H, benzoyl CONH), 8.09 (s, 1H, 5H), 8.31 (m, 1H, phthaloyl CONH). Anal. ($C_{29}H_{29}N_7O_6$·0.6AcOH·1.2H_2O) C, H, N.

Methyl 2-L-[*N*-[4-[*N*-[(2,4-Diamino-5-methylquinazolin-6-yl)methyl]amino]benzoyl]amino]-5-phthalimidopentanoate (37). A suspension of **32**[15a] (300 mg, 0.76 mmol), **34**[22] (453 mg, 2.3 mmol), and Raney Ni (0.4 g) in glacial AcOH (60 mL) was shaken under H_2 (1 atm) in a Parr apparatus for 18 h. The catalyst was removed by filtration through Celite, and the filter cake was washed with glacial AcOH. The combined filtrates were concentrated to 10 mL by rotary evaporation, then diluted with H_2O (40 mL), and adjusted to pH 9 with 28% NH_4OH. The precipitate was collected by centrifugation, washed with H_2O, and dried on a lyophilizer. The residue was chromatographed on a silica gel colum (30 g, 2 × 28 cm) with 95:5 and 92:8 $CHCl_3$−MeOH as the eluents. Fractions giving a single TLC spot with R_f 0.15 (silica gel, 100:10:1 $CHCl_3$−MeOH−28% NH_4OH) were pooled and evaporated. The residue was taken up in a small volume of 9:1$CHCl_3$−MeOH, the solution added dropwise with stirring to a large volume of Et_2O, and the precipitate collected and dried in vacuo at 60 °C over P_2O_5 to obtain **37** as a yellow powder (90 mg, 20%): mp 201−203 °C. Anal. ($C_{31}H_{31}N_7O_5$·1.4H_2O).

***N*$^{\alpha}$-[4-[*N*-[(2,4-Diamino-5-methylquinazolin-6-yl)methyl]amino]benzoyl]-*N*$^{\delta}$-hemiphthaloyl-L-ornithine (14).** A stirred solution of **37** (50 mg, 0.086 mmol) in DMSO (0.5 mL) was treated with 2 N NaOH (0.13 mL), and after 5 min the mixture was diluted with H_2O (7.5 mL) and adjusted to pH 4.2 with 10% AcOH. The precipitate was filtered, washed with H_2O (50 mL), and dried in a lyophilizer and then in vacuo at 60 °C over P_2O_5 to obtain a white powder (38 mg, 75%): mp 230 °C dec; TLC R_f 0.5 (5:4:1 $CHCl_3$−MeOH−28% NH_4OH); HPLC 16 min (C_{18} silica gel, 10% MeCN in 0.1 M NH_4OAc, pH 7.5, 1 mL/min); IR (KBr) ν 3360, 2950, 1610, 1380, 1330, 1270, 1190, 835, 770 cm^{-1}; UV (pH 7.4) λ_{max} 225 (ϵ 42 900), 294 (22 800) nm; ^1H NMR (DMSO-d_6) δ 1.51−1.93 (m, 4H, β- and γ-CH_2), 2.65 (s, 3H, 5-Me), 3.2 (m, 2H, δ-CH_2), 4.28 (m, 3H, α-CH and 9-CH_2), 6.55 (m, 2H, 3′- and 5′-H), 6.58 (m, 1H, 10-NH), 7.12 (d, 1H, 7H), (d, 1H, 8-H), 7.39−7.40 (m, 3H, phthaloyl), 7.50−7.52 (m, 1H, phthaloyl), 7.65−7.66 (m, 2H, 2′- and 6′-H), 7.99 (m, 1H, benzoyl CONH), 8.32 (m, 1H, phthaloyl). Anal. ($C_{30}H_{30}N_7O_6$·1.4H_2O) C, H, N.

Methyl 2-L-[*N*-[4-[*N*-[(2,4-Diamino-5-chloroquinazolin-6-yl)methyl]amino]benzoyl]amino]-5-phthalimidopentanoate (38). A slurry of Raney Ni (100 mg, 50% in H_2O) was added to a solution of **32**[15a] (200 mg, 0.51 mmol) and **35**[22] (166 mg, 0.76 mmol) in glacial AcOH (10 mL), and the mixture was stirred under a H_2-filled balloon at atmospheric pressure for 2 h. An additional portion of **35** (150 mg, 0.68 mmol) was then added, and stirring under H_2 was resumed for 2 h. The reaction mixture was filtered through Celite, the filter pad was washed with 15% AcOH, and the filtrate was cooled in an ice bath and neutralized with 28% NH_4OH. The precipitate was collected and chromatographed on silica gel with 100:10:1 CH_2Cl_2−MeOH−28% NH_4OH as the eluent. TLC homogeneous fractions were pooled and evaporated, and the gummy residue was recrystallized from hot EtOH to obtain **38** as a pale-yellow powder (122 mg, 43%): mp 209−211 °C. Anal. ($C_{30}H_{28}ClN_7O_5$·1.3H_2O) C, H, N.

***N*$^{\alpha}$-[4-[*N*-[(2,4-Diamino-5-chloroquinazolin-6-yl)methyl]amino]benzoyl]-*N*$^{\delta}$-hemiphthaloyl-L-ornithine (15).** A solution of **38** (110 mg, 0.18 mmol) in DMSO (1.5 mL) was treated with 2.5 N NaOH (0.2 mL) and stirred at room temperature for 5 min. The reaction mixture was diluted with H_2O (10 mL) and adjusted to pH 4.2 with 1 N HCl. The cream-colored precipitate was filtered and washed with H_2O (50 mL). The product was purified by ion-exchange on a DEAE-cellulose column (HCO_3^- form, 30 g, 300 × 18 mm) using 0.2 and 0.4 M NH_4HCO_3 (300 mL each) as eluents. TLC homogeneous fractions were pooled and kept in a lyophilizer for 4 days and then in vacuo at 60 °C over P_2O_5 for 2 days to obtain a pale-yellow solid (89 mg, 73%): mp 190−194 °C; IR (KBr) ν 3430, 2920, 1660, 1630, 1605, 1580, 1525, 1445, 1400, 1275, 1190, 830, 765 cm^{-1}; UV (pH 7.4) λ_{max} 237 (ϵ 40 200), 286 (24 500) nm; ^1H NMR (DMSO-d_6) δ 1.50−1.87 (m, 4H, β- and γ-CH_2), 3.13−3.31 (m, 2H, δ-CH_2), 4.29−4.32 (m, 1H, α-CH), 4.36 (d, 2H, 9-CH_2), 6.32 (broad s, 2H, NH_2), 6.55 (d, 2H, 3′- and 5′-H), 6.81 (m, 1H, 10-NH), 7.15 (d, 1H, 7-H), 7.36 (d, 1H, 8-H), 7.43−7.71 (m, 3H, 2′- and 6′-H, phthaloyl), 7.56 (broad s, 2H, NH_2), 7.64−7.71 (m, 3H, phthaloyl), 8.06 (d, 1H, phthaloyl CONH), 8.26 (m, 1H, benzoyl CONH). Anal. ($C_{30}H_{28}ClN_7O_5$·0.4H_2O) C, H, N.

Acknowledgment. This work was supported in part by Grants CA25394 and CA70349 from the National Cancer Institute, DHHS.

Supporting Information Available: IR and ^{1}H NMR spectral data for compounds **21**, **23**−**25**, **31**, **37**, and **38** (2 pages). Ordering information is given on any current masthead page.

References

(1) Rosowsky, A. Development of nonpolyglutamatable DHFR inhibitors. In *Antifolate Drugs: Basic Research and Clinical Practice*; Jackman, A. L., Ed.; Humana Press: Totowa, NJ; in press.

(2) (a) Matsuoka, H.; Ohi, N.; Mihara, M.; Suzuki, H.; Miyamoto, K.; Maruyama, N.; Tsuji, K.; Kato, N.; Akimoto, T.; Takeda, Y.; Yano, K.; Kuroki, T. Antirheumatic agents: Novel methotrexate derivatives bearing a benzoxazine moiety. *J. Med. Chem.* **1997**, *40*, 105−111. (b) Mihara, M.; Takagi, N.; Urakawa, K.; Moriya, Y.; Takeda, Y. Preventive effect of a novel antifolate, MX-68, in murine systemic lupus erythematosis (SLE). *Int. J. Immunopharmacol.* **1997**, *19*, 67−74.

(3) Kokuryo, Y.; Kawata, K.; Nakatani, T.; Kugimiya, A.; Tamura, Y.; Kawada, K.; Matsumoto, M.; Suzuki, R.; Kuwabara, K.; Hori, Y.; Ohtani, M. Synthesis and evaluation of novel fluorinated methotrexate derivatives for application to rheumatoid arthritis treatment. *J. Med. Chem.* **1997**, *40*, 3280−3291.

(4) Rosowsky, A.; Forsch, R.; Uren, J.; Wick, M.; Kumar, A. A.; Freisheim, J. H. Methotrexate analogues. 20. Replacement of glutamate by longer-chain amino diacids: Effects on dihydrofolate reductase inhibition, cytotoxicity, and in vivo antitumor activity. *J. Med. Chem.* **1983**, *26*, 1719−1724.

(5) (a) Li, E.-W.; Lin, J. T.; Tong, W. P.; Trippett, T. M.; Brennan, M. F.; Bertino, J. R. Mechanisms of natural resistance to antifolates in human soft tissue sarcomas. *Cancer Res.* **1992**, *52*, 1434−1438. (b) Li, W.-W.; Lin, J. T.; Schweitzer, B. I.; Tong, W. P.; Niedzwicki, D.; Bertino, J. R. Intrinsic resistance to methotrexate in human soft tissue sarcoma cell lines. *Cancer Res.* **1992**, *52*, 3908−3913.

(6) (a) Pizzorno, G.; Chang, Y. M.; McGuire, J. J.; Bertino, J. R. Inherent resistance of human squamous carcinoma cell lines to methotrexate as a result of decreased polyglutamylation of this drug. *Cancer Res.* **1989**, *49*, 5275−5280. (b) van Der Laan, B. F. A. M.; Jansen, G.; Kathmann, G. A. M.; Westerhof, G. R.; Schornagel, J. H.; Hordijk, G. J. In vitro activity of novel antifolates against human squamous carcinoma cell lines of the head and neck with inherent resistance to methotrexate. *Int. J. Cancer* **1992**, *51*, 909−914.

(7) Barakat, R. R.; Li, W.-W.; Lovelace, C.; Bertino, J. R. Intrinsic resistance of cervical squamous cell carcinoma cell lines to methotrexate (MTX) as a result of decreased accumulation of intracellular MTX polyglutamates. *Gynecol. Oncol.* **1993**, *51*, 54−60.

(8) (a) Whitehead, V. M.; Rosenblatt, D. S.; Vuchich, M.-J.; Shuster, J. J.; Witte, A.; Beaulieu, D. Accumulation of methotrexate and methotrexate polyglutamates in lymphoblasts at diagnosis of childhood acute lymphoblastic leukemia; A pilot prognostic factor analysis. *Blood* **1990**, *76*, 44−49. (b) Lin, J. T.; Tong, W. P.; Trippett, T. M.; Nidzwiecki, D.; Tao, Y.; Tan, C.; Steinherz, P.; Schweitzer, I.; Bertino, J. R. Basis for natural resistance to methotrexate in human acute nonlymphocytic leukemia. *Leukemia Res.* **1991**, *15*, 1191−1196. (c) Barredo, J. C.; Synold, T. W.; Laver, J.; Relling, M. V.; Pui, C.-C.; Priest, D. G.; Evans, W. E. Differences in constitutive and post-methotrexate folylpolyglutamate synthetase activity in B-lineage and T-lineage leukemia. *Blood* **1994**, *84*, 564−569. (d) Galpin, A. M.; Schuetz, J. D.; Masson, E.; Yanishevski, Y.; Synold, T. E.; Barredo, J. C.; Pui, C.-H.; Relling, M. V.; Evans, W. E. Differences in folylpolyglutamate synthetase and dihydrofolate reductase expression in human B-lineage versus T-lineage leukemic lymphoblasts: mechanisms for lineage differences in methotrexate polyglutamation and cytotoxicity. *Mol. Pharmacol.* **1997**, *52*, 155−163.

(9) (a) Rosowsky, A.; Bader, H.; Cucchi, C. A.; Moran, R. G.; Kohler, W.; Freisheim, J. H. Methotrexate analogues. 33. N^{δ}-Acyl-N^{α}-(4-amino-4-deoxypteroyl)-L-ornithine derivatives: synthesis and in vitro antitumor activity. *J. Med. Chem.* **1988**, *31*, 1322−1337. (b) Rosowsky, A.; Bader, H.; Forsch, R. A. Synthesis of the folylpolyglutamate synthetase inhibitor N^{α}-pteroyl-L-ornithine and its N^{δ}-benzoyl and N^{δ}-hemiphthaloyl derivatives, and an improved synthesis of N^{α}-(4-amino-4-deoxypteroyl)-N^{δ}-hemiphthaloyl-L-ornithine. *Pteridines* **1989**, *1*, 91−98.

(10) Westerhof, G. R.; Schornagel, J. H.; Kathmann, I.; Jackman, A. L.; Rosowsky, A.; Forsch, R. A.; Hynes, J. B.; Boyle, F. T.; Peters, G. J.; Pinedo, H. M.; Jansen, G. Carrier- and receptor-mediated transport of folate antagonists targeting folate-dependent enzymes: correlates of molecular structure and biological activity. *Mol. Pharmacol.* **1995**, *48*, 459−471.

(11) Rhee, M. S.; Galivan, J.; Wright, J. E.; Rosowsky, A. Biochemical studies on PT523, a potent nonpolyglutamatable antifolate, in cultured cells. *Mol. Pharmacol.* **1994**, *45*, 783−791.

(12) Johnson, J. M.; Meiering, E. M.; Wright, J. E.; Pardo, J.; Rosowsky, A.; Wagner, G. NMR solution structure of the antitumor compound PT523 and NADPH in the ternary complex with human dihydrofolate reductase. *Biochemistry* **1997**, *36*, 4399−4411.

(13) Cody, V.; Galitsky, N.; Luft, J. R.; Pangborn, W.; Rosowsky, A.; Blakley, R. L. Comparison of two independent crystal structures of human dihydrofolate reductase ternary complexes with reduced nicotinamide adenine dinucleotide phosphate and the very tight-binding inhibitor PT523. *Biochemistry* **1997**, *36*, 13897−13903.

(14) (a) Klohs, W. D.; Steinkampf, R. W.; Besserer, J. A.; Fry, D. A. Cross resistance of pleiotropically drug resistant P388 leukemia cells to the lipophilic antifolates trimetrexate and BW301U. *Cancer Lett.* **1986**, *31*, 253−260. (b) Ramu, N.; Ramu, A.; Cole, D. E.; Balis, F. M.; Poplack, D. G.; Pollard, H. B. Mechanism of acquired resistance to methotrexate in P388 cells and in their doxorubicin-resistant subline. *Israel J. Med. Sci.* **1988**, *24*, 477−482. (c) Assaraf, Y. G.; Molina, A.; Schimke, R. T. Cross-resistance to the lipid-soluble antifolate trimetrexate in human carcinoma cells with the multidrug-resistant phenotype. *J. Natl. Cancer Inst.* **1989**, *81*, 290−294.

(15) (a) Rosowsky, A.; Bader, H.; Wright, J. E.; Keyomarsi, K.; Matherly, L. H. Synthesis and biological activity of N^{ω}-hemiphthaloy-α,ω-diaminoalkanoic acid analogues of aminopterin and 3′,5′-dichloroaminopterin. *J. Med. Chem.* **1994**, *37*, 2167−2174. (b) Rosowsky, A.; Vaidya, C. M.; Bader, H.; Wright, J. E.; Teicher, B. A. Analogues of N^{α}-(4-amino-4-deoxy)-N^{δ}-hemiphthaloyl-L-ornithine (PT523) modified in the side chain: synthesis and biological evaluation. *J. Med. Chem.* **1997**, *40*, 286−299.

(16) (a) Allegra, C. J.; Drake, J. C.; Jolivet, J.; Chabner, B. A. Inhibition of phosphoribosyl-aminoimidazolecarboxamide transformylase by methotrexate and dihydrofolic acid polyglutamates. *Proc. Natl. Acad. Sci. U.S.A.* **1985**, *82*, 4881−1885. (b) Allegra, C. J.; Chabner, B. A.; Drake, J. C.; Lutz, R.; Rodbard, D.; Jolivet, J. Enhanced inhibition of thymidylate synthase by methotrexate polyglutamates. *J. Biol. Chem.* **1985**, *260*, 9720−9726.

(17) Rosowsky, A.; Forsch, R. A.; Bader, H.; Freisheim, J. H. Synthesis and in vitro biological activity of new deaza analogues of folic acid, aminopterin, and methotrexate with an L-ornithine side chain. *J. Med. Chem.* **1991**, *34*, 1447−1454.

(18) Piper, J. E.; McCaleb, G. S.; Montgomery, J. A.; Kisliuk, R. L.; Gaumont, Y.; Sirotnak, F. M. Syntheses and antifolate activity of 5-methyl-5-deaza analogues of aminopterin, methotrexate, folic acid, and N^{10}-methylfolic acid. *J. Med. Chem.* **1986**, *29*, 1080−1087.

(19) An alternative route to **18** and **19** would be to condense 4-aminobenzoic acid with 2,4-diamino-6-(bromomethyl)pyrido-[2,3-*d*]pyrimidines; see: Piper, J. R.; Malik, N. D.; Rhee, M. S.; Galivan, J.; Sirotnak, F. M. Synthesis and antifolate evaluation of the 10-propargyl derivatives of 5-deazafolic acid, 5-deazaaminopterin, and 5-methyl-5-deazaaminopterin. *J. Med. Chem.* **1992**, *35*, 332−337.

(20) Srinivasan, A.; Broom, A. Pyridopyrimidines. 12. Synthesis of 8-deaza analogues of aminopterin and folic acid. *J. Org. Chem.* **1981**, *46*, 1777−1781.

(21) An improved method of preparation of **26**·HBr was subsequently developed; see: Rosowsky, A.; Forsch, R. A.; Queener, S. F. 2,4-Diaminopyrido[3,2-*d*]pyrimidine inhibitors of dihydrofolate reductase from *Pneumocystis carinii* and *Toxoplasma gondii*. *J. Med. Chem.* **1995**, *38*, 2615−2620.

(22) Davoll, J.; Johnson, A. M. Quinazoline analogues of folic acid. *J. Chem. Soc.* **1970**, 997.

(23) Prendergast, N. J.; Delcamp, T. J.; Smith, P. L.; Freisheim, J. H. Expression and site-directed mutagenesis of human dihydrofolate reductase. *Biochemistry* **1988**, *27*, 3664- 3671.

(24) Appleman, J. R.; Prendergast, N.; Delcamp, T. J.; Freisheim, J. H.; Blakley, R. L. Kinetics of the formation and isomerization of methotrexate complexes of recombinant human dihydrofolate reductase. *J. Biol. Chem.* **1988**, *263*, 10304−10313.

(25) Henderson, P. J. F. A linear equation that describes the steady-state kinetics of enzymes and subcellular particles interacting with tightly bound inhibitors. *Biochem. J.* **1972**, *127*, 321−333.

(26) Jackson, R. C.; Hart, L. I.; Harrap, K. R. Intrinsic resistance to methotrexate of cultured mammalian cells in relation to the inhibition kinetics of their dihydrofolate reductases. *Cancer Res.* **1976**, *36*, 1991−1997.

(27) Sirotnak, F. M.; Schmid, F. A.; Otter, G. M.; Piper, J. R.; Montgomery, J. A. Structural design, biochemical properties, and evidence for improved therapeutic activity of 5-alkyl derivatives of 5-deazaminopterin and 5-deazamethotrexate compared to methotrexate in murine tumor models. *Cancer Res.* **1988**, *48*, 5686−5691.

(28) Rosowsky, A.; Forsch, R. A.; Queener, S. F.; Bertino, J. R. Synthesis of 2,4-diaminopteridines with bulky lipophilic groups at the 6-position as inhibitors of *Pneumocystis carinii*, *Toxoplasma gondii*, and mammalian dihydrofolate reductase. *Pteridines* **1997**, *8*, 173−187.

(29) Chen, G.; Wright, J. E.; Rosowsky, A. Dihydrofolate reductase binding and cellular uptake of nonpolyglutamatable antifolates: correlates of cytotoxicity toward methotrexate-sensitive and -resistant human head and neck squamous carcinoma cells. *Mol. Pharmacol.* **1995**, *48*, 758−765.

(30) Monks, A.; Scudiero, D.; Skehan, P.; Shoemaker, R.; Paull, K.; Vistica, D.; Hose, C.; Langley, J.; Cronise, P.; Vaigro-Wolff, A.; Gray-Goodrich, M.; Campbell, H.; Mayo, J.; Boyd, M. Feasibility of a high-flux anticancer drug screen using a diverse panel of cultured human tumor cell lines. *J. Natl. Cancer Inst.* **1991**, *83*, 757−766.

(31) (a) Stinson, S. F.; Alley, M. C.; Kopp, W. C.; Fiebig, H.-H.; Mullendore, L. A.; Pittman, A. F.; Kenney, S.; Keller, J.; Boyd, M. R. Morphological and immunocytochemical characteristics of human tumor cell lines for use in a disease-oriented anticancer drug screen. *Anticancer Res.* **1992**, *12*, 1035−1054. (b) Wu, L.; Smythe, A. M.; Stinson, S. F.; Mullendore, L. A.; Monks, A.; Scudiero, D. A.; Paull, K. D.; Koutsoukos, A. D.; Rubinstein, L. V.; Boyd, M. R.; Schoemaker, R. H. Multidrug-resistant phenotype of disease-oriented panels of human tumor cell lines used for anticancer drug screening. *Cancer Res.* **1992**, *52*, 3029−3034. (c) Moscow, J. A.; Connolly, T.; Myers, T. G.; Cheng, C. C.; Paull, K.; Cowan, K. H. Reduced folate carrier gene (*RFC*1) expression and antifolate resistance in transfected and nonselected cell lines. *Int. J. Cancer* **1997**, *72*, 184−190. (d) O′Connor, P. M.; Jackman, J.; Bae, I.; Myers, T. G.; Fan, S.; Mutoh, M.; Scudiero, D. A.; Monks, A.; Sausville, E. A.; Weinstein, J. D.; Friend, S.; Fornace, A. J.; Kohn, K. W. Characterization of the p53 tumor suppressor pathway in cell lines of the NCI anticancer drug screen and correlations with the growth inhibitory potency of 123 anticancer agents. *Cancer Res.* **1997**, *57*, 4285−4300.

(32) Sirotnak, F. M.; Chello, P. L.; DeGraw, J. I.; Piper, J. R.; Montgomery, J. A. Membrane transport and the molecular basis for selective antitumor action of folate analogues. In *Molecular Actions and Targets for Cancer Chemotherapeutic Agents*; Sartorelli, A. C., Lazo, J. S., Bertino, J. R., Eds.; Academic Press: New York, 1981; pp 349−384.

(33) Kuehl, M.; Brixner, D. I.; Broom, A. D.; Avery, T. L.; Blakley, R. L. Cytotoxicity, uptake, polyglutamate formation, and antileukemic effects of 8-deaza analogues of methotrexate and aminopterin in mice. *Cancer Res.* **1988**, *48*, 1481−1488.

(34) Susten, S. S.; Hynes, J. B.; Kumar, A.; Freisheim, J. H. Inhibition of dihydrofolate reductase, methotrexate transport, and growth of methotrexate-sensitive and -resistant L1210 leukemia cells in vitro by 5-substituted 2,4-diaminoquinazolines. *Biochem. Pharmacol.* **1985**, *34*, 2163−2167.

(35) Coll, R. J.; Cesar, D.; Hynes, J. B.; Shane, B. In vitro metabolism of 5,8-dideazafolates and 5,8-dideazaisofolates by mammalian folylpoly-γ-glutamate synthetase. *Biochem. Pharmacol.* **1991**, *42*, 833−838.

(36) Rosowsky, A.; Freisheim, J. H.; Bader, H.; Forsch, R. A.; Susten, S. S.; Cucchi, C. A.; Frei, E., III. Methotrexate analogues. 25. Chemical and biological studies on the γ-*tert*-butyl esters of methotrexate and aminopterin. *J. Med. Chem.* **1985**, *28*, 660−667.

JM980477+